# Estimating Cotton Crop Water Use from Multispectral Aerial Imagery

G.J. Fitzgerald, D.J. Hunsaker, E.M. Barnes, T.R. Clark, S.M. Lesch, R. Roth, P.J. Pinter, Jr.

## Abstract

Precision irrigation can improve field-scale water use by improving timing and placement of water. However, current numerical models used for irrigation scheduling rely on single point measurements to predict irrigation needs for entire fields. To incorporate the spatial dimension, imaging remote sensing approaches were investigated in Central Arizona for estimating water use by cotton growing in a furrow-irrigated field with large variation in soil texture. Aerial imagery was obtained every two to three weeks using a high resolution camera system equipped with narrow band-pass filters and calibrated with ground-based reference tarps. A directed sampling approach was used to establish optimal locations to install neutron access tubes and estimate canopy height and width for use in calculating basal crop coefficients ($K_{cb}$). The normalized difference vegetation index (NDVI) was used to estimate $K_{cb}$ for cotton via a previously defined relationship. The $K_{cb}$ plus estimated soil evaporation coefficients were multiplied by reference evapotranspiration ($ET_o$) determined from a nearby weather station and summed during each irrigation interval to provide water use maps. These maps were validated using soil water balance with periodic soil moisture measurements. The study demonstrated how maps showing the spatial and temporal dynamics of crop water use can offer insight into effects of soil properties and crop response and help define and manage zones in surface irrigated fields.

## Introduction

Precision irrigation requires a measure of spatial variability, but it is not feasible to measure the parameters needed to calculate crop coefficients at every location in a field. The use of surrogate crop coefficients for evapotranspiration (ET) estimation based on remotely sensed imagery could provide the needed spatial dimension. If a relationship between the imagery and the ground data needed for estimating crop coefficients could be established, then the imagery could be converted to water-use image-maps.

Remote sensing can be used to infer plant and soil characteristics. Vegetation indices (VI), such as the normalized difference vegetation index (NDVI), have been shown to relate to many crop parameters (Moran et al., 1997), including canopy width and height. The NDVI is defined as the ratio of reflected energy in the near-infrared (NIR) and red parts of the spectrum: [NIR-red]/ [NIR+red]. The potential for using VIs as surrogates for crop coefficients was proposed many years ago by Jackson et al. (1980). This approach has been further developed as described by Hunsaker et al. (2003b) where they also discuss the use of NDVI for estimating the basal crop coefficient ($K_{cb}$) in cotton in the same field described in this study. The objective of this study was to use a previously established relationship between NDVI and $K_{cb}$ along with soil water depletion and local meteorological data to produce a seasonal water-use map of a cotton field.

## Materials and Methods

### Description of field and location

The experimental site was a 3.4-ha field planted to cotton (*Gossypium hirsutum* L., cv Delta Pine 448B) on 15 April, 2002 at the University of Arizona's Maricopa Agricultural Center (MAC) located approximately 40 km south of Phoenix (33º 04' 21" N; 111º 58' 45" W) at an elevation of 360 m. The field straddles the transition between two soil series (Post et al., 1988): Mohall sandy loam (fine-loamy, mixed, hyperthermic Typic Haplargid) is dominant on the northeast portion of the field, and Casa Grande sandy clay loam (fine-loamy, mixed, hyperthermic Typic Natrargids) spans most of the southwest region (Fig. 1). This is an arid area, receiving only 185 mm of rainfall per year with daily summer temperatures ranging from 25° to 46°C. The field had an on-going tillage study imposed with 4-row “skips” where no cotton was grown. The field was furrow irrigated from the east.

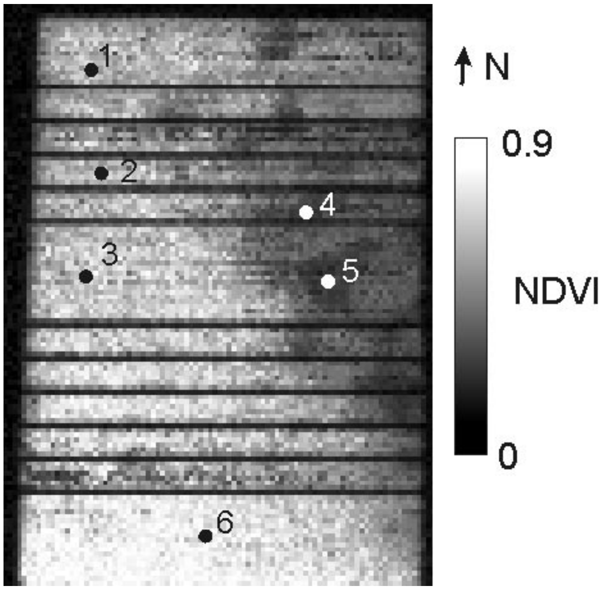

Figure 1. Mid-season normalized difference vegetation index (NDVI) of field with neutron access tube locations indicated. Dark to light pixels represent low to high NDVI values. Low NDVI values indicate areas of sparse, shorter cotton plants with visible soil background while higher values indicate larger, vigorous plants and full canopy. The diagonal NW to SE feature is the dividing line for two soil types, one with a higher sand content on the NE side of the field. The E to W dark lines are skip rows where cotton was not planted.

### Remote Sensing

In 2002, imagery was acquired (Table 1) on nine dates at two to three week intervals using a Duncan MS3100 camera that acquired three coincident, 8-bit images in three wavebands. The wavebands were centered on 670 nm, 720 nm, and 790 nm with a 10-nm bandwidth. Flight altitudes were 1070 m (3500 ft.) above ground level and the camera had a 15º X 20º field of view resulting in a pixel resolution of about 0.3 m. Calibrated reflectance tarps (Group VIII Technologies, Provo, UT) were placed in a nearby field during each flight, and images were acquired within 7 minutes of acquiring images of the tarps. Coincident, ground-based radiometer measurements were taken over the tarps and other targets for use in calibration of the imagery to reflectance. These procedures and calibration tarps are similar to those described by Moran et al. (2001). Geometric registration was accomplished by measuring coordinates of markers place in the images with a Trimble Ag114 receiver with real-time differential correction.

### Sampling and Image Processing

Neutron access tube locations were chosen based on a directed sampling study in this field the previous year. Directed sampling provides a measure of field variability from measurements at fewer locations as compared to grid sampling, and it can be more cost effective (Pocknee, 1996). Additionally, canopy height and width were

Table 1. Flight numbers and dates, planting date, and Day of Year (DOY).

| Flight No. | Date (2002) | DOY |
|---|---|---|
| Planting | 15 Apr | 105 |
| 1 | 21 May | 141 |
| 2 | 12 Jun | 163 |
| 3 | 25 Jun | 176 |
| 4 | 11 Jul | 192 |
| 5 | 26 Jul | 207 |
| 6 | 13 Aug | 225 |
| 7 | 3 Sep | 246 |
| 8 | 18 Sep | 261 |
| 9 | 1 Oct | 274 |

not measured at the neutron access tube locations but were collected in other locations of the field. Canopy height and width were, however, estimated at the locations of the six neutron access tubes (Fig. 1) for use in calculation of $K_{cb}$ using the following procedures.

A statistical procedure developed by Lesch et al. (1995a, b) and implemented in the ESAP-RSSD (ECe Sampling, Assessment, and Prediction – Response Surface Sampling Design) software package was originally written to generate optimal soil sampling designs from bulk soil electrical conductivity survey information by selecting a minimum set of calibration samples based on the observed magnitudes and spatial locations of the data, with the explicit goal of optimizing the estimation of a linear regression model. The regression model is then used to predict all remaining (i.e., non-sampled) areas. The default setting in the ESAP-RSSD program selects 12 georegistered calibration locations for sampling, thus directing the user to these locations. In this study, the ESAP-RSSD program was used to direct ground sampling based on aerial Normalized Difference Vegetation Index (NDVI) images as input rather than electromagnetic induction data. The NDVI images were first converted to reflectance using the above-mentioned ground tarps and procedures and georegistered. Ground sampling based on the ESAP-RSSD results was conducted shortly after image acquisitions, usually within 24 hours. Data collected from the ESAP-RSSD directed ground locations were used to calibrate the images to produce canopy width and height image-maps of the field. Neutron access tube locations were measured with a differentially-corrected global positioning system (DGPS) and located in these georeferenced image-maps. Mean pixel values were extracted from the imagery in 2-m diameter areas around the canopy height and width locations and neutron tubes for use in developing $K_{cb}$ curves. The 2-m diameter size was chosen as representative of the ground sampling area because this corresponded to the canopy height width measurement areas and DGPS data were accurate to within plus or minus 1 m, or 2-m diameter.

The ESAP-RSSD software requires that the data meet some assumptions in order to produce accurate sampling designs (Lesch et al., 1995a, b):

1) The covariate data (NDVI) must represent a dense grid.
2) A linear relationship must exist between the primary attributes (canopy height and width) and the covariate.
3) The residuals of the regression model between the primary attribute and covariate must be spatially uncorrelated.

The images acquired provide a dense grid where every location in the field was effectively sampled. A linear relationship was shown to exist between canopy height and width but is not presented here. The ESAP-RSSD software generates a design that optimizes the sampling locations by choosing spatially distributed and uncorrelated locations. Thus, the assumptions for use of the ESAP-RSSD software were met with the use of NDVI images and supporting ground data. Canopy height and width were accurately interpolated to the neutron access tube locations. These locations were spatially uncorrelated and a simple regression model could relate NDVI to canopy height and width.

### Ground Sampling

At each location identified by the ESAP-RSSD procedure, plant height and canopy width were measured. Plant height was measured by placing a 2-m long rod on the soil surface and measuring the height of plants at each 0.5-m interval in two adjacent 1.02-m (40-in.) rows. The mean was taken as the plant height for each location. Canopy width was measured along this 2-m length by visually estimating the canopy edges and measuring across the row.

A neutron access tube and TDR waveguide were installed in the middle of a cotton bed at each of the six locations based on the previous year's ESAP-RSSD sampling design. Volumetric soil water contents were measured at each location beginning on 29 May 2002 using neutron scattering and time-domain-reflectometry (TDR) techniques. Soil water content for the 0 to 0.3-m soil layer was measured with the TDR, and at 0.2 m increments to a soil depth of 2.0 m with a site-calibrated neutron probe. Usually, soil water measurements were made the day before and three days after each irrigation. However, there were occasions during the season when irrigation water was applied before the water content measurements could be made at the locations. Following the termination of irrigation in mid-August, water contents were measured approximately once a week at all six sites until the crop was defoliated.

### ET and $K_{cb}$ Estimations

Cumulative cotton evapotranspiration (ET) for each of the six locations was calculated as the soil water balance residual (eq. 1) for time periods between two successive soil water measurement dates:

$$ET = (\theta_1 - \theta_2)\, Rd + I + R - DP \qquad (1)$$

where $\theta_1$ and $\theta_2$ are the volumetric water contents of the effective rooting depth on the first and second date of sampling, respectively, in $m^3\ m^{-3}$, Rd is effective crop root depth in mm, I is the depth of irrigation in mm, R is rainfall in mm, and DP is deep percolation below the root zone in mm. The change in soil water storage was determined for a soil depth of 1.7 m, the estimated maximum Rd for cotton (Allen et al., 1998). However, cumulative ET was not determined from the water balance for periods when irrigation occurred between two successive soil water measurement dates due to large uncertainties in the amount of water applied and subsequent drainage below the root zone. Consequently, seasonal cumulative ET for each site was determined as the summation of cumulative ET that was measured from the soil water balance for periods when irrigation was not applied, and estimations for cumulative ET for the periods when irrigation was applied. The estimation procedures used for determining cumulative ET for non-measured periods were presented by Hunsaker (1999, pp 929-930), but will be briefly described below.

For each site, basal crop coefficients ($K_{cb}$) were derived for the periods of measured cumulative ET (typically 7 to 9 days long) using the FAO-56 dual crop coefficient procedures (Allen et al., 1998). The dual crop coefficient relationship to ET can be defined as follows:

$$ET = (K_{cb}K_s + K_e)\ ET_o \tag{2}$$

where ET and grass reference evapotranspiration ($ET_o$) are cumulative amounts for the period in mm, $K_{cb}$ is the basal crop coefficient, $K_s$ is the water stress reduction coefficient, and $K_e$ is the soil water evaporation coefficient. For eq. 2, ET is known from the soil water balance, and $ET_o$ is known, as calculated using local meteorological data within the FAO-56 $ET_o$ equation (Allen et al., 1998). Assuming that the values for $K_{cb}$ for each day of a given period were constant, daily FAO-56 calculations for $K_s$ and $K_e$ were made for the days within the period. The $K_{cb}$ value was repeatedly adjusted until the right side of eq. 2 calculated the same cumulative ET as the measured cumulative ET for the period. Daily values of $K_{cb}$ for periods between measurement periods (i.e., periods with irrigation) were then estimated by linear interpolation based on measured $K_{cb}$ values immediately before and after the period in question (Fig. 2). The FAO-56 calculations were made to estimate the daily ET for those unmeasured periods. Prior to the first measurement period (early June), a cotton $K_{cb}$ of 0.15 was assumed for the first 30 days for all sites, based on the FAO-56 $K_{cb}$ guideline for cotton. Interpolation of daily $K_{cb}$ was then made from the 31st day to the first measured $K_{cb}$ for each individual site. Soil and other parameters used for the FAO-56 calculations are listed in Hunsaker et al. (2003b, Table 2) with two exceptions. Values for canopy height (h) and fraction of soil surface covered by vegetation ($f_c$) were estimated from calibrations developed between measured values and NDVI for each of the nine overflights. Daily values for h and $f_c$ were interpolated between the parameter estimates for successive overflight dates.

Predicted daily ET as a function of days past planting (DPP) for each of the six neutron access tubes was calculated with the FAO-56 dual crop coefficient procedures but using daily $K_{cb}$ values determined from a previously defined relationship between $K_{cb}$ and NDVI for cotton (Hunsaker et al., 2003a, b). The relationship consisted of two regression relations: a linear function used from early vegetative growth to effective full cover (NDVI=0.8), and a multiple regression of $K_{cb}$ as a function of NDVI and cumulative growing-degree-days (GDD) after effective full cover. The $K_{cb}$ values were restricted to 0.15 or larger. Daily values for NDVI for each location were interpolated from observations made during the nine overflights. Using the linear regression developed between cumulative NDVI and the predicted cumulative ET at the neutron access tube locations (Fig. 3), a seasonal cumulative water-use map was generated (Fig. 4).

Root Mean Square Error (RMSE) and coefficient of determination ($r^2$) values were calculated from a regression derived from the nine measured versus predicted ET values for the cumulative ET measured periods (Fig. 2 and Table 2).

## Results and Discussion

The processes in this field were dominated by soil variability because of the two soil types present. Thus, ET and water-use were expected to vary. Neutron access tube locations 1, 2, 3, and 6 (see Fig. 1) showed similar patterns in $K_{cb}$ between the measured and predicted seasonal curves (Fig. 2). The periods between about 80 and 120 days past planting (DPP) showed higher values of $K_{cb}$ for the predicted model, but no ground data were collected during this period and the measured values do not follow the predicted. These locations were in parts of the field with vigorous plant growth and development (see Fig. 1). Points 4 and 5 were located in parts of the field with smaller plants where the canopy never closed completely, and the soil had more sand. The predictive model under-predicted the measured $K_{cb}$ at these "sparse" locations early in the season (Fig. 2). The model was developed for cotton grown on a different soil, and the Kcb-NDVI relationship may have been different in this field. The model does not increase $K_{cb}$ from the minimum value of 0.15 until an NDVI value of 0.2 is reached.

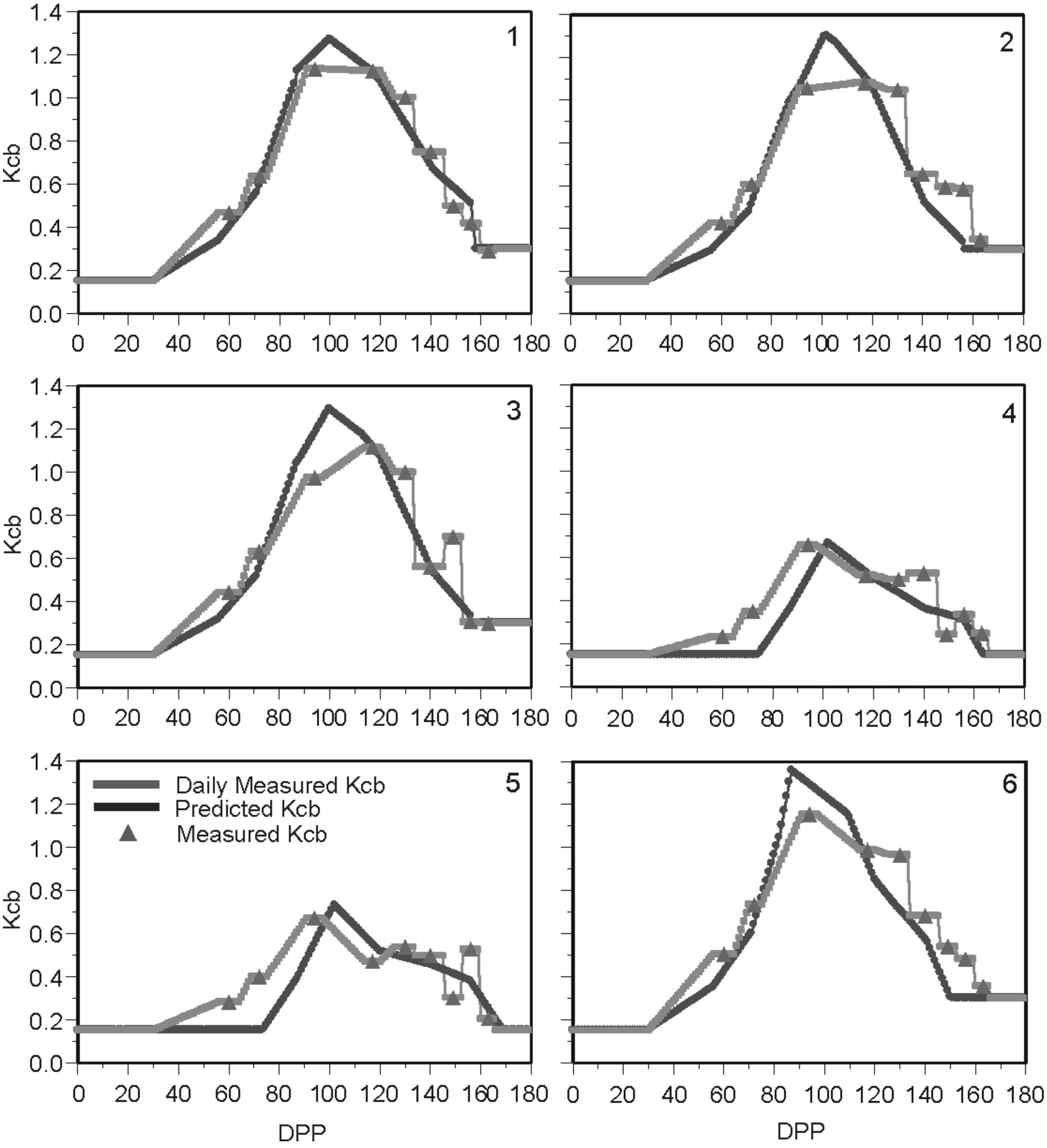

Figure 2. Days Past Planting (DPP) vs. basal crop coefficient ($K_{cb}$) at each of the six neutron access tube locations (1-6). Predicted $K_{cb}$ values were estimated from a previously defined relationship with NDVI and is discussed in the text. Daily measured $K_{cb}$ was calculated with soil moisture measurements from neutron access tubes and interpolated between the dates using FAO-56 procedures. The actual measured $K_{cb}$ values are indicated by triangles and are in the middle of the measured cumulative ET periods.

Table 2. Root mean square error (mm) and coefficient of determination ($r^2$) for the cumulative measured ET (mm) periods derived from regressing the measured versus predicted ET values (see text). Mean predicted ET (mm) is presented as a comparison for the RMSE values. These are summarized by location across the nine measured cumulative ET periods and by period across the six neutron access tube locations. Day of year (DOY) shows the day of the midpoint of the each of these periods.

| Location | Mean Pred. (mm) | RMSE (mm) | $r^2$ |
|---|---|---|---|
| 1 | 342 | 3.6 | 0.97*** |
| 2 | 303 | 5.6 | 0.93*** |
| 3 | 313 | 6.6 | 0.91*** |
| 4 | 158 | 4.5 | 0.81*** |
| 5 | 186 | 6.5 | 0.69*** |
| 6 | 316 | 7.3 | 0.90*** |

| Measured Cumulative ET Period | DOY | Mean Pred. (mm) | RMSE (mm) | $r^2$ |
|---|---|---|---|---|
| 1 | 165 | 23.8 | 1.6 | 0.98*** |
| 2 | 177 | 25.5 | 1.9 | 0.98*** |
| 3 | 199 | 52.2 | 4.5 | 0.96*** |
| 4 | 222 | 50.4 | 3.1 | 0.97*** |
| 5 | 234 | 36.9 | 2.9 | 0.93*** |
| 6 | 244 | 43.8 | 5.7 | 0.66* |
| 7 | 254 | 13.7 | 3.7 | 0.03 ns |
| 8 | 261 | 15.1 | 2.8 | 0.01 ns |
| 9 | 267 | 8.5 | 1.4 | 0.36 ns |

* $p < 0.05$, ** $p < 0.01$, *** $p < 0.001$

The NDVI did not reach 0.2 until relatively late (about 75 DPP), so the model did not increase $K_{cb}$ appropriately. It is well established that soil background color can have a strong influence on NDVI (Huete, 1988). One possible solution would be to use another vegetation index, such as the soil-adjusted vegetation index (Huete, 1988) to develop a relationship with $K_{cb}$ and correct for sparse areas in the field.

The seasonal cumulative ET ($ET_s$) in mm vs. seasonal cumulative NDVI ($NDVI_s$) for all six neutron access tubes (Fig. 3) showed a strong relationship for ET calculated from the predicted $K_{cb}$ values in Fig. 2. The measured $ET_s$ based on the daily measured $K_{cb}$ showed good correlation to the predicted $K_{cb}$ for the higher values corresponding to the vigorous locations 1, 2, 3, and 6. The regression under-predicted $ET_s$ at the sparse locations 4 and 5 because predicted $K_{cb}$ was under-predicted early in the season, as discussed above. The y-intercept shows evaporation for bare soil over the season and corresponds well with the value of 235 mm obtained using the FAO-56 procedure by setting $K_{cb} = 0$.

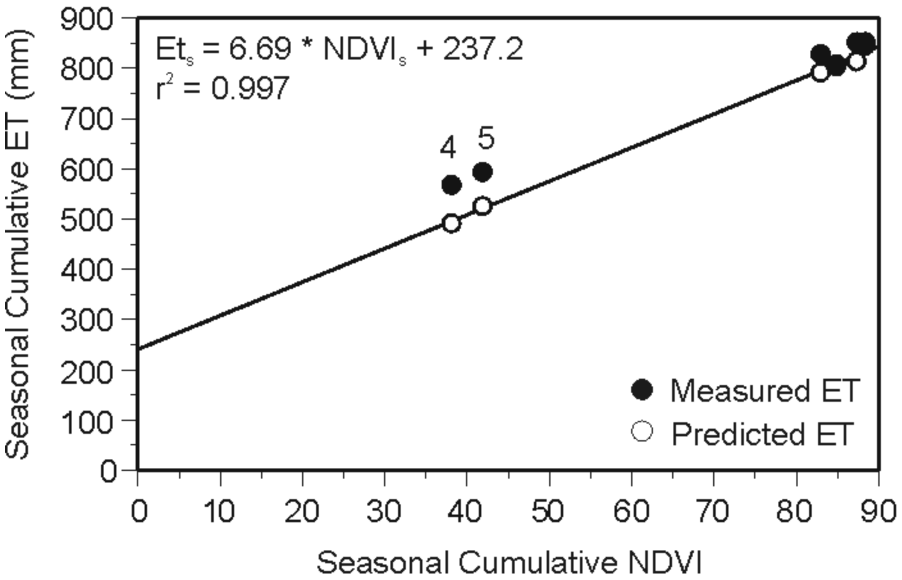

Figure 3. Seasonal cumulative NDVI ($NDVI_S$) vs. predicted (open circles & regression line) and measured (closed circles) cumulative ET ($ET_S$) in mm. The time period for calculating the cumulative values was DOY 141 to DOY 274, the dates between the first and last aerial image acquisitions. The measured ET values are the actual seasonal cumulative values measured at the six neutron probe locations (with interpolation between dates) and the predicted values are those estimated from the FAO-56 model described in the text for the neutron probe locations. The value of 237 mm at the y-intercept indicates estimated evaporation from a bare soil surface. Data from the sparse locations 4 and 5 are indicated.

For each location across all dates, the predictive power was quite strong for the vigorous locations (Table 2). At sparse locations 4 and 5, the $r^2$ values were highly significant but there was more scatter in the data. The RMSE values were about twice as high relative to the mean of the predictive model.

The RMSE and coefficients of determination for each of the nine measured cumulative ET periods and locations are separated out in Table 2. Within each period, there was a strong correlation between the measured and predicted ET for the first 5 periods. The RMSE values were within 9% of the mean for the predicted ET values for these periods, and the $r^2$ values were highly significant. Periods 6 to 9 showed weaker to poor correlations and greater RMSE relative to the predicted mean ET. This poor performance could have be due to a number of factors: 1) The original directed sampling locations for these dates were chosen based on other indices, not NDVI. The residuals for these points could have been spatially correlated when used to calculate NDVI and violated this assumption of the models upon which ESAP-RSSD is based. 2) NDVI and canopy height and width relationship became weaker later in the season as senescence began. 3) Periods 7 and 8 experienced significant rain events that were likely not uniformly distributed across the field and therefore difficult to accurately model. 4) The model accuracy decreased during the latter half of the season. The most likely causes of poor $r^2$ and higher RMSE values are points 3 and 4 above. Noteworthy is that the $r^2$ of periods 7 and 8 were basically zero.

The seasonal cumulative water-use map (Fig. 4) was arbitrarily divided into four levels to represent bare soil and three levels of crop water-use. Not surprisingly, it looks like the mid-season NDVI image in Fig. 1. As stated earlier, biophysical functions in this field were controlled by soil features. The black values represent

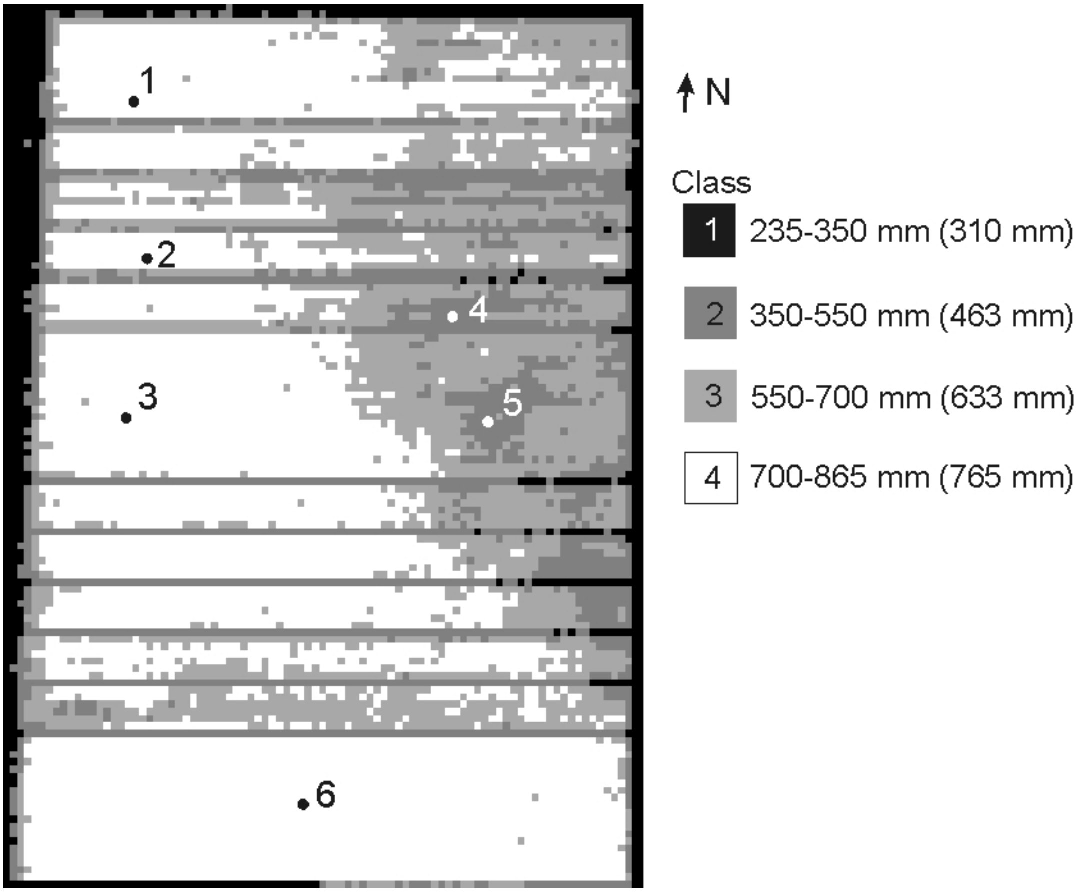

Figure 4. Seasonal cumulative water use map. The four classes represent values from low to high seasonal water use. The values in parentheses are the means for each level. The lowest value, 235 mm represents the amount of water lost during the season from soil evaporation. The values were based on those predicted at the neutron access tube locations and extrapolated to all other locations by using the equation presented in Fig. 3 relating cumulative NDVI to cumulative ET. See text for details. The six numbered points show the locations of the neutron access tubes. The spatial patterns clearly show soil differences and skip rows.

bare or almost bare soil and encompass the field edges and some of the skip row areas. Class 2 shows the sandier soil and corresponds to the locations of neutron access tubes 4 and 5, in the sparse areas. Class 3 shows predominantly sandy areas but along with class 2, occupies the skip row areas. Although there were no plants in the skip rows, pixel averaging to 2-m resolution created pixels with values combining soil and plant characteristics along these edges. The areas of greatest water-use are shown in white, and occurred over the less sandy soil. There also may have been some influence due to management as seen in the lower sections of Fig. 4 where point 6 was located. An on-going tillage trial tested the effects of various methods of soil incorporation for cotton stubble. This may have influenced the crop, producing vigorous plants in the most southern section of the field and less vigorous plants in the two narrow sections just north of this because of treatment differences.

## Summary and Conclusions

Combining remote sensing with predictive models of ET can allow the temporal modeling approach to be interpolated across the spatial dimension. A combination of sampling design, ground sampling, image acquisition and processing, and computer modeling is needed to expand the use of ET models for precision irrigation. Additionally, the approach demonstrated here allows sampling of only a few ground locations lowering the acquisition cost of otherwise expensive “ground truthing”.

## Disclaimer

Mention of specific suppliers of hardware and software in this manuscript is for informative purposes only and does not imply endorsement by the United States Department of Agriculture.

## Literature Cited

Allen R.G., L.S. Pereira, D. Raes, M. Smith. 1998. Crop evapotranspiration. FAO Irrigation and Drainage Paper 56, Food and Agricultural Organization of the United Nations, Rome.

Huete, A.R. A Soil-Adjusted Vegetation Index (SAVI). 1988. Remote Sensing of Environment. 25:295-309.

Hunsaker D.J. 1999. Basal crop coefficients and water use for early maturity cotton. Trans. ASAE 42(4):927-936.

Hunsaker D.J., P.J. Pinter Jr., E.M. Barnes, B.A. Kimball. 2003a. Estimating cotton evapotranspiration crop coefficients with a multispectral vegetation index. Irrigation science (in press).

Hunsaker, D.J., P.J. Pinter, Jr., G.J. Fitzgerald, and T.R. Clarke. 2003b. Tracking spatial and temporal cotton ET patterns with a normalized difference vegetation index. *In*: 24th IA International Conference, San Diego 18-20 Nov. (this edition).

Jackson, R.D., S.B. Idso, R.J. Reginato, P.J. Pinter, Jr. 1980. Remotely sensed crop temperatures and reflectances as inputs to irrigation scheduling. *In*: Drain Spec. Conf. Proc., 23-25 July, Boise, ID, ASCE, New York, pp 390-397.

Lesch, S.M., D.J. Strauss, J.D. Rhoades. 1995a. Spatial prediction of soil salinity using electromagnetic induction techniques, 1. Statistical prediction models: A comparison of multiple linear regression and co-kriging. Water Resources Res., 31: 387-398.

Lesch, S.M., D.J. Strauss, J.D. Rhoades. 1995b. Spatial prediction of soil salinity using electromagnetic induction techniques, 2. An efficient spatial sampling algorithm suitable for multiple linear regression model identification and estimation. Water Resources Res., 31: 387-398.

Moran, M. S., Y. Inoue, and E.M. Barnes. 1997. Opportunities and Limitations for Image-Based Remote Sensing and Precision Crop Management. Remote Sensing of Environment, 61:319-346.

Moran, M. S., R. Bryant, T.R. Clarke, and J. Qi. 2001. Deployment and calibration of reference reflectance tarps for use with airborne cameras. *Photogrammetric Engineering and Remote Sensing* 67:273-286.

Pocknee, S., B.C. Boydell, H.M. Green, D.J. Waters, and C.K. Kvien. 1996. Directed soil sampling. *In* Proc. 3rd Int. Conf. on Precision Agriculture, P.C. Robert, R.H. Rust, and W.E. Larson (eds.), pp 159-168, Madison, WI: ASA.

Post, D.F., C. Mack, P.D. Camp, A.S. Sulliman. 1988. Mapping and characterization of the soils on the University of Arizona, Maricopa Agricultural Center. *In*: Proc. of Hydrology and Water Resources in Arizona and the Southwest. Univ. of Arizona, Tucson, AZ, pp. 49-60.